

Aerobic Oxidative Esterification of Aldehydes with Alcohols by Gold–Nickel Oxide Nanoparticle Catalysts with a Core–Shell Structure

Ken Suzuki,^{*†} Tatsuo Yamaguchi,[‡] Ken Matsushita,[‡] Chihiro Itsuka,[‡] Junichi Miura,[‡] Takayuki Akaogi,[‡] and Hiroshi Ishida[‡]

[†]R&D Planning and Business Development, Asahi Kasei Chemicals Corporation, 1-105 Kanda Jinbocho, Chiyoda-ku, Tokyo 101-0051, Japan

[‡]Catalyst Laboratory, Asahi Kasei Chemicals Corporation, 2767-11 Niihama Shionasu Kojima, Kurashiki, Okayama 711-8510, Japan

Supporting Information

ABSTRACT: Oxidative esterification of aldehydes with alcohols proceeds with high efficiency in the presence of molecular oxygen on supported gold–nickel oxide (AuNiO_x) nanoparticle catalysts. The method is environmentally benign because it requires only molecular oxygen as the terminal oxidant and gives water as the side product. The AuNiO_x nanoparticles have a core–shell structure, with the Au nanoparticles at the core and the surface covered by highly oxidized NiO_x . Aerobic oxidative esterification of methacrolein in methanol to methyl methacrylate is an important industrial method for the production of polymethyl methacrylate.



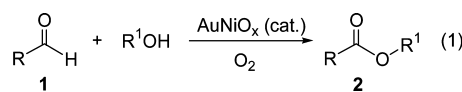
KEYWORDS: gold, nickel oxide, nanoparticle, core–shell, aerobic oxidation, esterification

Esterification, one of the most fundamental transformations in organic synthesis, is widely used in laboratories and industries.¹ Esterification of aldehydes with alcohols is an attractive method for the synthesis of esters because aldehydes are raw materials that are readily available on a commercial scale. Although several facile and selective esterification reactions have been reported,² the development of a catalytic method for the direct oxidative esterification of aldehydes with alcohols under mild and neutral conditions in the presence of molecular oxygen as the terminal oxidant is highly desirable for both economic and environmental reasons.

Since Haruta et al. discovered that highly dispersed Au nanoparticles supported on reducible and catalytically active supports such as Fe_2O_3 , Co_3O_4 , TiO_2 , and NiO oxides have exceptionally high activity for CO and H_2 oxidation,³ Au-catalyzed oxidation reactions have been widely investigated. Efforts are being directed at achieving highly selective oxidation using molecular oxygen.⁴ Several Au-nanoparticle-based catalysts for the aerobic esterification of aldehydes⁵ or alcohols⁶ have been reported. In this paper, we report a highly selective and efficient catalytic method for the oxidative esterification of aldehydes with alcohols that employs supported gold–nickel oxide (AuNiO_x) nanoparticles as the catalyst and molecular oxygen as the terminal oxidant (Scheme 1).

As an example, the aerobic catalytic esterification of methacrolein **1a** with methanol to form methyl methacrylate (MMA; **2a**) was investigated under neutral conditions. The

Scheme 1. Oxidative Esterification of Aldehydes with Alcohols in the Presence of Molecular Oxygen Using Supported Gold–Nickel Oxide (AuNiO_x) Nanoparticles As the Catalyst



monomer MMA is used mainly to produce acrylic plastics, such as poly(methyl methacrylate) (PMMA) and other polymer dispersions used in paints and coatings. MMA can be manufactured in numerous ways from C_2 – C_4 hydrocarbon feedstocks.⁷ Currently, MMA is produced mainly via the acetone cyanohydrin process, but there are problems in handling the resulting ammonium bisulfate waste and toxic hydrogen cyanide. Some manufacturers use isobutene or *tert*-butyl alcohol as the starting material, which is sequentially oxidized first to methacrolein and then to methacrylic acid, which in turn is esterified with methanol. Recently, an environmentally benign procedure based on the use of molecular oxygen and a Pd–Pb catalyst has been developed for the direct oxidative esterification of methacrolein with

Received: May 30, 2013

Revised: July 16, 2013

Published: July 17, 2013

methanol to yield MMA.⁸ This work was an important milestone in the aerobic oxidative esterification of aldehydes because it put forth a clean and efficient method of forming carboxylic esters. However, the existing synthetic methods still suffer from several disadvantages; methods for successful catalytic oxidative esterification are limited because selective oxidation of methacrolein is extremely difficult because of the instability of α,β -unsaturated aldehydes. Therefore, the development of an efficient and highly selective catalytic system based on the above reaction remains a challenge.

Table 1 summarizes the activity of various catalysts used in the aerobic esterification of **1a** with methanol. The activity of

Table 1. Catalytic Activity for Aerobic Oxidative Esterification of Methacrolein (1a**) with Methanol To Form Methyl Methacrylate^a**

entry	catalyst	conversion of aldehyde 1a (%) ^b	selectivity for ester 2a (%) ^b
1 ^c	Pd/SiO ₂ –Al ₂ O ₃	20	40
2 ^c	PdPb/SiO ₂ –Al ₂ O ₃	34	84
3	AuNiO _x /SiO ₂ –Al ₂ O ₃ –MgO	58	98
4	AuNiO _x /SiO ₂ –Al ₂ O ₃	63	97
5	AuNiO _x /SiO ₂ –TiO ₂	29	96
6	Au/SiO ₂ –Al ₂ O ₃ –MgO	14	91
7	Au/SiO ₂ –Al ₂ O ₃	17	79
8	Au/SiO ₂ –TiO ₂	6	89
9	AuNi/SiO ₂ –Al ₂ O ₃ –MgO	12	89

^aReaction conditions: **1a** (containing 50 ppm hydroquinone inhibitor, 15 mmol), catalyst (Au: 0.1 mol %) in methanol (10 mL), O₂/N₂ (7:93 (v/v), 3 MPa) at 60 °C for 2 h. ^bDetermined by GC analysis using tetradecane as an internal standard. ^cPd-based catalyst (Pd: 0.5 mol %).

previously reported Pd catalysts was investigated first.⁸ When 2.5 wt % Pd/SiO₂–Al₂O₃ was used, **2a** could not be obtained in satisfactory yields (entry 1) because the decarbonylation of **1a** resulted in the formation of large amounts of propylene and CO₂ as byproducts. When oxidative esterification was carried out by the addition of Pb(OAc)₂ to the reaction mixture, decarbonylation was inhibited, and the selectivity to **2a** improved to 84% (entry 2). The active species in the above reaction was found to be the intermetallic compound Pd₃Pb₁. During oxidative esterification in the presence of methanol, the excess methanol is oxidized to form methyl formate (MF) as a byproduct (0.2 mols of MF per mole of MMA). The turnover number (TON) of the catalyst, defined as the total number of moles of the product **2a** formed per mole of the Pd catalyst, was determined to be 61. Attempts to carry out esterification of **1a** to **2a** in the presence of other Pd-based catalysts were unsuccessful.

We then turned our attention to nickel oxide. Nickel peroxide is known to be highly oxidizing and can stoichiometrically oxidize various alcohols.⁹ The catalytic aerobic oxidation of alcohols was possible after the recent development of catalysts such as Ni–Al hydrotalcite and nanosized NiO₂ powder.^{10,11} Nickel peroxide was also found to participate in oxidative esterification of aldehydes with alcohols.¹² We

examined the relationship between the chemical form and reactivity and developed a new catalytic system of composite nanoparticles composed of NiO and Au active species.

Au and NiO were supported on SiO₂–Al₂O₃–MgO (average particle size, 60 μ m) by coprecipitation. The amounts of Au and Ni in the supported nanoparticle were determined to be 0.9 and 1.1 wt %, respectively, by inductively coupled plasma–atomic emission spectroscopy (ICP–AES). Thus, the reaction of **1a** in the presence of AuNiO_x/SiO₂–Al₂O₃–MgO in methanol at 60 °C under an oxygen–nitrogen mixture (7:93 (v/v), 3 MPa, outside flammability limits) for 2 h gave **2a** with 98% selectivity and 58% conversion (entry 3). On the basis of the moles of MMA formed per mole of the Au catalyst, the TON of the supported nanoparticle catalyst was determined to be 621, and its activity was ~10 times that of the Pd–Pb catalyst. Moreover, reduced byproduct (MF) formation was observed in this case (0.007 mols of MF formed per mole of MMA). Oxidative esterification was found to proceed with high efficiency, even when SiO₂–Al₂O₃ and SiO₂–TiO₂ were used as carriers (entries 4 and 5). The catalyst supported with only Au nanoparticles showed lower activity and selectivity than the supported AuNiO_x catalyst (entries 6–8). The activity and selectivity of the Au–Ni catalyst, prepared by reduction of the AuNiO_x catalyst under H₂ atmosphere at 400 °C for 3 h, was greatly decreased (entry 9). The oxidative esterification activity of the AuNiO_x catalyst showed a strong dependence on the Au and NiO composition in the supported nanoparticle. The maximum activity was observed for 20 mol % of Au (Figure 1).

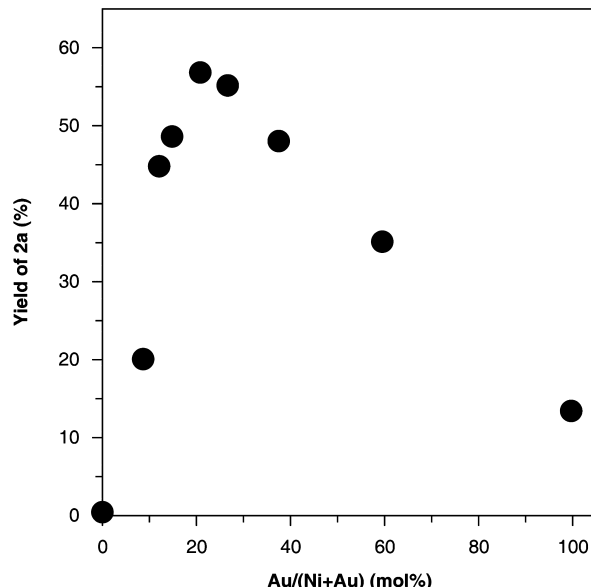


Figure 1. Yield of methyl methacrylate **2a** during the oxidative esterification of methacrolein **1a** in methanol over catalysts with varying Au/Ni compositions.

Next, oxidative esterification of various aldehydes and alcohols was carried out by using the AuNiO_x catalyst (Table 2). When oxidative esterification of **1a** was carried out in the presence of AuNiO_x/SiO₂–Al₂O₃–MgO in methanol at 80 °C, under an oxygen–nitrogen mixture (7:93 (v/v), 3 MPa) for 1 h, **2a** was obtained with 98% selectivity and 62% conversion (entry 1). The conversion of benzaldehyde **1b** to methyl benzoate **2d** was highly efficient (entry 4). When oxidative esterification of **1a** and **1b** was carried out using ethanol and *n*-

Table 2. AuNiO_x -Catalyzed Aerobic Oxidative Esterification of Aldehydes with Alcohols^a

entry	aldehyde	alcohol	product	conversion (%) ^b / selectivity (%) ^b
1		methanol		62/98
2		ethanol		11/97
3		<i>n</i> -butanol		15/97
4		methanol		61/97
5		ethanol		10/97

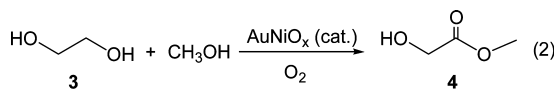
^aReaction conditions: aldehyde (containing 50 ppm hydroquinone inhibitor, 15 mmol), $\text{AuNiO}_x/\text{SiO}_2\text{--Al}_2\text{O}_3\text{--MgO}$ (Au: 0.1 mol %) in alcohol (10 mL), O_2/N_2 (7:93 (v/v), 3 MPa) at 80 °C for 1 h.

^bDetermined by GC analysis using tetradecane as an internal standard.

butanol in place of methanol, the corresponding esters (**2b**, **2c**, and **2e**) were obtained with high selectivity but with lower conversion efficiencies than those in the case of using methanol (entries 2, 3, and 5), presumably due to steric effects.

The oxidative esterification of alcohols to afford the corresponding esters was also highly efficient. When oxidative esterification of ethylene glycol **3** was carried out in methanol at 90 °C, under an oxygen–nitrogen mixture (7:93 (v/v), 3 MPa) for 4 h, methyl glycolate **4** was obtained with 95% selectivity and 39% conversion (Scheme 2).

Scheme 2. Oxidative Esterification of Ethylene Glycol **3** in Methanol



Spherical particles of the AuNiO_x catalyst that are uniformly distributed on the carrier can be seen in the transmission electron microscopy (TEM) images (Figure 2a, b). The particles have a diameter of 2–3 nm (number-average particle diameter: 3.0 nm). Size distribution histograms of the particles are shown in Figure S1 (Supporting Information). High-magnification images revealed a lattice of Au (111) particles with a *d* spacing of 2.36 Å. Elemental analysis of individual particles by energy-dispersive X-ray (EDX) spectroscopy showed the presence of Ni and Au in the particles. The average Ni/Au atomic ratio of the nanoparticles was 0.82 (100 units used for calculation). As shown in Figure 2c–d, EDX analysis was performed on the scanning transmission electron microscopy (STEM) image of the nanoparticles. The results showed that the Ni/Au atomic ratio was 0.73 at the center of the particle (Figure 2c, measurement point 1) but 2.95 at the edge of the particle (Figure 2c, measurement point 2). Trace amounts of Ni were detected in areas that did not contain the particle (Figure 2c, measurement point 3). On the basis of the composition profile observed in the direction of the scan, Ni appears to be more widely distributed than Au (Figure 2d). Thus, Ni was distributed on the Au particles as well as around

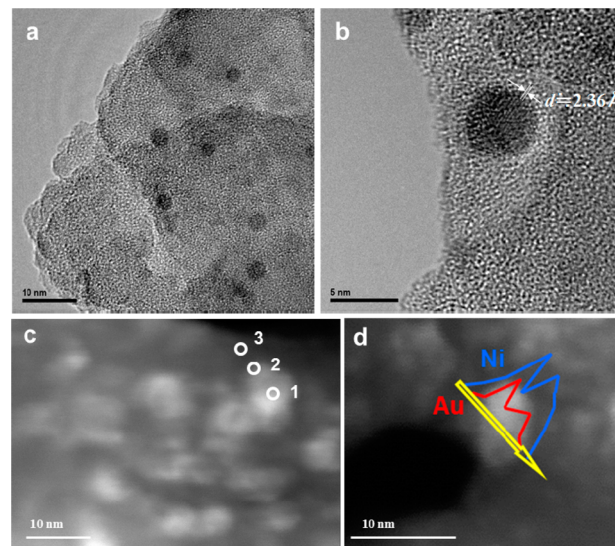


Figure 2. (a, b) Typical transmission electron microscopy images of the $\text{AuNiO}_x/\text{SiO}_2\text{--Al}_2\text{O}_3\text{--MgO}$ catalyst. (c) Point analysis and (d) line analysis of the energy-dispersive X-ray images of the supported catalyst obtained by scanning transmission electron microscopy.

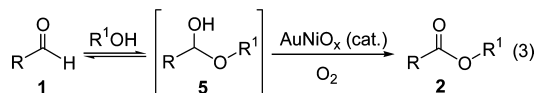
the edges of the particles. Hence, it was assumed that the surface of the Au particles is covered by Ni without alloy formation. However, TEM/STEM images of the Ni shell around the Au particles could not be obtained.

A broad diffraction peak attributable to Au^0 was observed in X-ray diffraction (XRD) patterns. The absence of diffraction peaks due to Ni suggested that Ni existed as a noncrystalline phase (Figure S2, Supporting Information). The Au 4f and Ni 2p XPS spectra confirmed the oxidation states of Au and Ni to be 0 and +2, respectively (Figure S3, Supporting Information). When the variation in the electronically excited state was examined using ultraviolet–visible (UV–vis) spectroscopy, no surface plasmon absorption peak, as observed in the case of the Au catalyst, originated from the Au nanoparticles (~ 530 nm) in the case of the AuNiO_x catalyst (Figure S4, Supporting Information). The AuNiO_x catalyst was brown and showed a broad absorption peak in the wavelength region 200–800 nm. The spectrum pattern and color of the catalyst were similar to those of $\text{NiO}_x/\text{SiO}_2\text{--Al}_2\text{O}_3\text{--MgO}$, synthesized by the oxidation of $\text{NiO}/\text{SiO}_2\text{--Al}_2\text{O}_3\text{--MgO}$ using NaOCl . Thus, it can be deduced that the surface electronic state of the AuNiO_x catalyst differs from that of the Au-only catalyst as Ni was present in a highly oxidized state.

The representative Fourier transform-infrared (FT-IR) spectra of CO adsorbed on the catalysts are shown in Figure S5 (Supporting Information). The Au catalyst showed an intense band attributed to $\text{Au}^0\text{-CO}$, at 2058 cm^{-1} .¹³ In contrast, the AuNiO_x catalyst showed only a weak signal attributed to $\text{Ni}^{2+}\text{-CO}$, at 2111 cm^{-1} .¹⁴ No peak corresponding to $\text{Au}^0\text{-CO}$ could be observed. On the basis of these results, the AuNiO_x nanoparticle was assumed to have a core–shell structure with Au nanoparticle at the core and its surface covered by highly oxidized NiO_x . NiO exists in a highly oxidized state in the AuNiO_x catalyst owing to heterometallic bonding interactions with Au (ligand effect). In control experiments, nickel peroxide was found to show catalytic activity in oxidative esterification reactions. Therefore, we suggest that the active species in this case are the highly oxidized NiO_x supported on Au. The oxidative esterification of

aldehydes can be rationalized by assuming Scheme 3. A condensation reaction between **1** and an alcohol results in the formation of hemiacetal **5**, which undergoes oxidative dehydrogenation to give **2**.

Scheme 3. Reaction Pathway for the Oxidative Esterification of Aldehydes via the Formation of Hemiacetal **5 as the Key Intermediate**



Stability and long life are the key requirements of an effective catalyst. We precisely controlled the distribution of AuNiO_x nanoparticles in the catalyst to decrease any loss of metals and to achieve high activity. Loss of metals from catalyst can occur because of detachment or abrasion under reaction. The AuNiO_x layer was sharply distributed in a region within a 10- μ m depth from the catalyst surface layer, and AuNiO_x was shifted by submicrometer from the surface of the catalyst to inside (Figure 3). The catalytic life of AuNiO_x/SiO₂–Al₂O₃–

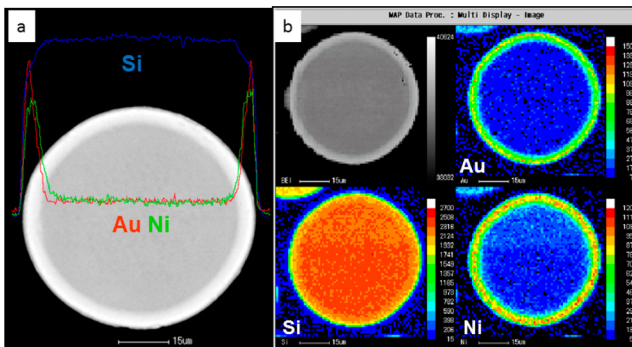
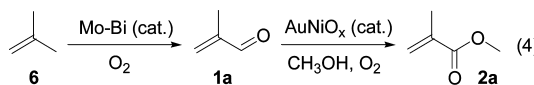


Figure 3. Electron-probe microanalysis spectra of a single particle of AuNiO_x/SiO₂–Al₂O₃–MgO. (a) Secondary electron image and line analysis. (b) Color mapping display corresponding to the concentration of element distribution.

MgO was evaluated by using a continuous-flow reaction apparatus (Figure S6, Supporting Information). When the conversion efficiency of the reaction was maintained at \sim 60%, **2a** was obtained with high selectivity (96–97%). No decrease in the catalyst activity was observed over a period of 1000 h. Furthermore, metal leaching was negligible during prolonged reactions. The concentration of Au and Ni in the reaction mixture was determined to be <2.5 ppb by ICP-AES. TEM observation of the catalyst after the reaction showed no sintering of the AuNiO_x nanoparticles. The TEM/STEM-EDX, UV-vis, and FT-IR results confirmed that the core–shell structure of AuNiO_x was preserved.

The practical applicability of this catalytic system was verified in a 100 000 ton/year MMA production plant. Thus, isobutene **6** was oxidized in the gaseous phase using a Mo–Bi catalyst to synthesize **1a**. Subsequent oxidative esterification of **1a** in the presence of methanol using the AuNiO_x catalyst produced **2a** (Scheme 4). This process confirmed the high selectivity, high activity, and long life of the AuNiO_x catalyst. This catalyst would help in saving energy and resources, in addition to being highly economical.

Scheme 4. Reaction Studied for Assessing the Practical Applicability of Our Catalytic System



In conclusion, we have developed novel supported AuNiO_x nanoparticles having a core–shell structure that can efficiently catalyze the aerobic oxidative esterification of aldehydes with alcohols under mild and neutral reaction conditions. This strategy provides an efficient and environmentally benign method for the synthesis of esters. We are currently working on the reaction mechanism and with the aim of possibly extending this catalysis system to other oxidation reactions.

ASSOCIATED CONTENT

Supporting Information

Details of the experimental procedures and characterization results. This material is available free of charge via the Internet at <http://pubs.acs.org.org>.

AUTHOR INFORMATION

Corresponding Author

*E-mail: suzuki.kd@om.asahi-kasei.co.jp.

Notes

The authors declare no competing financial interest.

REFERENCES

- Otera, J. *Esterification: Methods, Reaction and Applications*; Wiley-VCH: Weinheim, Germany, 2003.
- Dehydrogenation: (a) Murahashi, S.-I.; Naota, T.; Ito, K.; Maeda, Y.; Taki, H. *J. Org. Chem.* **1987**, *52*, 4319–4327. Oxidation with hydrogen peroxide: (b) Gopinath, R.; Patel, B. K. *Org. Lett.* **2000**, *2*, 577–579. (c) Wu, X.-F.; Darcel, C. *Eur. J. Org. Chem.* **2009**, 1144–1147. (d) Gopinath, R.; Barkakaty, B.; Talukdar, B.; Patel, B. K. *J. Org. Chem.* **2003**, *68*, 2944–2947. Oxidation with TBHP: (e) Hashmi, A. S. K.; Lothschuetz, C.; Ackermann, M.; Doepp, R.; Anantharaman, S.; Marchetti, B.; Bertagnolli, H.; Rominger, F. *Chem.—Eur. J.* **2010**, *16*, 8012–8019. Oxidation with benzyl chloride: (f) Liu, C.; Tang, S.; Zheng, L.; Liu, D.; Zhang, H.; Lei, A. *Angew. Chem., Int. Ed.* **2012**, *51*, 5662–5666. Review: (g) Ekoue-Kovi, K.; Wolf, C. *Chem.—Eur. J.* **2008**, *14*, 6302–6315.
- (a) Haruta, M.; Kobayashi, T.; Sano, H.; Yamada, N. *Chem. Lett.* **1987**, 405–408. (b) Haruta, M.; Yamada, N.; Kobayashi, T.; Iijima, S. *J. Catal.* **1989**, *115*, 301–309.
- Reviews: (a) Hashmi, A. S. K.; Hutchings, G. J. *Angew. Chem., Int. Ed.* **2006**, *45*, 7896–7936. (b) Arcadi, A. *Chem. Rev.* **2008**, *108*, 3266–3325. (c) Li, Z.; Brouwer, C.; He, C. *Chem. Rev.* **2008**, *108*, 3239–3265. (d) Pina, C. D.; Falletta, E.; Prati, L.; Rossi, M. *Chem. Soc. Rev.* **2008**, *37*, 2077–2095. (e) Corma, A.; Garcia, H. *Chem. Soc. Rev.* **2008**, *37*, 2096–2126.
- (a) Marsden, C.; Taarning, E.; Hansen, D.; Johansen, L.; Klitgaard, S. K.; Egeblad, K.; Christensen, C. H. *Green Chem.* **2008**, *10*, 168–170. (b) Fristrup, P.; Johansen, L. B.; Christensen, C. H. *Chem. Commun.* **2008**, 2750–2752. (c) Su, F.-Z.; Ni, J.; Sun, H.; Cao, Y.; He, H.-Y.; Fan, K.-N. *Chem.—Eur. J.* **2008**, *14*, 7131–7135. (d) Taarning, E.; Nielsen, L. S.; Egeblad, K.; Madsen, R.; Christensen, C. H. *ChemSusChem.* **2008**, *1*, 75–78. (e) Xu, B.; Liu, X.; Haubrich, J.; Friend, C. M. *Nat. Chem.* **2009**, *2*, 61–65.
- (a) Abad, A.; Concepcion, P.; Corma, A.; Garcia, H. *Angew. Chem., Int. Ed.* **2005**, *44*, 4066–4069. (b) Hayashi, T.; Inagaki, T.; Itayama, N.; Baba, H. *Catal. Today.* **2006**, *117*, 210–213. (c) Nielsen, I. S.; Taarning, E.; Egeblad, K.; Madsen, R.; Christensen, C. H. *Catal. Lett.* **2007**, *116*, 35–40. (d) Jorgensen, B.; Christiansen, S. E.; Thomsen, M. L. D.; Christensen, C. H. *J. Catal.* **2007**, *251*, 332–337.

(e) Zheng, N.; Stucky, G. D. *Chem. Commun.* **2007**, 3862–3864.
(f) Klitgaard, S. K.; Riva, A. T. D.; Helveg, S.; Werchmeister, R. M.; Christensen, C. H. *Catal. Lett.* **2008**, 126, 213–217. (g) Ishida, T.; Nagaoka, M.; Akita, T.; Haruta, M. *Chem.—Eur. J.* **2008**, 14, 8456–8460. (h) Su, F.-N.; Ni, J.; Sun, H.; Cao, Y.; He, H.-Y.; Fan, K.-N. *Chem.—Eur. J.* **2008**, 14, 7131–7135. (i) Oliveira, R. L.; Kiyohara, P. K.; Rossi, L. M. *Green Chem.* **2009**, 11, 1366–1370. (j) Casanova, O.; Iborra, S.; Corma, A. *J. Catal.* **2009**, 265, 109–116. (k) Miyamura, H.; Yasukawa, T.; Kobayashi, S. *Green Chem.* **2010**, 12, 776–778. (l) Parreira, L. A.; Bogdanchikova, N.; Pestryakov, A.; Zepeda, T. A.; Tuzovskaya, I.; Farias, M. H.; Gusevskaya, E. V. *Appl. Catal., A* **2011**, 397, 145–152. (m) Costa, V. V.; Estrada, M.; Demidova, Y.; Prosvirin, I.; Kriventsov, V.; Cotta, R. F.; Fuentes, S.; Simakov, A.; Gusevskaya, E. V. *J. Catal.* **2012**, 292, 148–156. (n) Kotionova, T.; Lee, C.; Miedziak, P.; Dummer, N. F.; Willock, D. J.; Carley, A. F.; Morgan, D. J.; Knight, D. W.; Taylor, S. H.; Hutchings, G. *J. Catal. Lett.* **2012**, 142, 1114–1120.
(7) Nagai, K. *Appl. Catal., A* **2001**, 221, 367–377.
(8) (a) Yamamatsu, S.; Yamaguchi, T.; Yokota, K.; Nagano, O.; Chono, M.; Aoshima, A. *Catal. Surv. Asia* **2010**, 14, 124–131. (b) Diao, Y.; Yan, R.; Zhang, S.; Yang, P.; Li, Z.; Wang, L.; Dong, H. *J. Mol. Catal. A: Chem.* **2009**, 303, 35–42. (c) Wang, B.; Sun, W.; Zhu, J.; Ran, W.; Chen, S. *Ind. Eng. Chem. Res.* **2012**, 51, 15004–15010.
(9) Nakagawa, K.; Konaka, R.; Nakata, T. *J. Org. Chem.* **1962**, 27, 1597–1601.
(10) (a) Choudary, B. M.; Kantam, M. L.; Rahman, A.; Reddy, Ch. V.; Rao, K. K. *Angew. Chem., Int. Ed.* **2001**, 40, 763–766. (b) Ji, H.; Wang, T.; Zhang, M.; She, Y.; Wang, L. *Appl. Catal., A* **2005**, 282, 25–30.
(11) In the field of electronic materials, research is being conducted on NiO–M (M: Ni, Pd, Pt, Au, Ag, Cu) composite film to quicken the light-absorption response of Ni oxide film used as an electrochromic material. The metal doped into Ni oxide is supposed to act as a positive hole and improves the speed of oxidative coloring by converting Ni oxide into a higher oxidation state. Ferreira, F. F.; Fantini, M. C. A. *J. Phys. D: Appl. Phys.* **2003**, 36, 2386–2392.
(12) The reaction of **1a** (15 mmol) in the presence of $\text{NiO}_2 \cdot n\text{H}_2\text{O}$ (0.3 g) in methanol at 80 °C under an oxygen–nitrogen mixture (7:93 (v/v), 3 MPa) for 2 h gave a trace of **2a** (1.5 μmol).
(13) Mihaylov, M.; Knoezinger, H.; Hadjiiivanov, K.; Gates, B. C. *Chem. Ing. Tech.* **2007**, 79, 795–806.
(14) Estrella Platero, E.; Scarano, D.; Zecchina, A.; Meneghini, G.; De Franceschi, R. *Surf. Sci.* **1996**, 350, 113–122.